Cell. Mol. Life Sci. (2016) 73:3761–3775
DOI 10.1007/s00018-016-2219-9

Cellular and Molecular Life Sciences

ORIGINAL ARTICLE

HspB5/αB-crystallin increases dendritic complexity and protects the dendritic arbor during heat shock in cultured rat hippocampal neurons

Britta Bartelt-Kirbach[1] · Margarethe Moron[1] · Maximilian Glomb[1] · Clara-Maria Beck[1] · Marie-Pascale Weller[1] · Nikola Golenhofen[1]

Received: 15 July 2015 / Revised: 18 March 2016 / Accepted: 5 April 2016 / Published online: 16 April 2016

Abstract The small heat shock protein HspB5 (αB-crystallin) exhibits generally cytoprotective functions and possesses powerful neuroprotective capacity in the brain. However, little is known about the mode of action of HspB5 or other members of the HspB family particularly in neurons. To get clues of the neuronal function of HspBs, we overexpressed several HspBs in cultured rat hippocampal neurons and investigated their effect on neuronal morphology and stress resistance. Whereas axon length and synapse density were not affected by any HspB, dendritic complexity was enhanced by HspB5 and, to a lesser extent, by HspB6. Furthermore, we could show that this process was dependent on phosphorylation, since a non-phosphorylatable mutant of HspB5 did not show this effect. Rarefaction of the dendritic arbor is one hallmark of several neurodegenerative diseases. To investigate if HspB5, which is upregulated at pathophysiological conditions, might be able to protect dendrites during such situations, we exposed HspB5 overexpressing neuronal cultures to heat shock. HspB5 prevented heat shock-induced rarefaction of dendrites. In conclusion, we identified regulation of dendritic complexity as a new function of HspB5 in hippocampal neurons.

Keywords Dendritic branching · Hippocampus · Neuroprotection · Small heat shock proteins · Stress tolerance

Introduction

Many organs, including the brain, exhibit powerful endogenous cytoprotective mechanisms to survive recurrent cellular stress events. In the brain, the development of stress tolerance has been reported in animal models as well as in retrospective case–control studies in humans [1–4]. Stress tolerance is a multifactorial process triggered by the cellular stress response and mediated mainly by the upregulation of heat shock proteins [5–7]. Upregulation of heat shock proteins also takes place in neurodegenerative diseases, which is presumably the response to chronic cellular stress conditions.

In this study, we investigated the group of small heat shock proteins characterized by their molecular weight between 12 and 43 kDa comprising ten family members called HspB1 to HspB10 [8]. HspB11 (PP25, IFT25) debated as an eleventh family member should not be included into the HspB family because of the lack of the characteristic α-crystallin domain [9, 10]. In rat brain, six HspBs (HspB1, HspB2, HspB3, HspB5, HspB6, and HspB8) are expressed with HspB2 and HspB3 restricted to some brain regions [11]. In the following, we will focus on HspB5, formerly named αB-crystallin. HspB5 was first identified in the eye lens being important for the refractive properties and lenticular transparency. Later, it has been studied extensively in the heart, where it shows high expression and its cardioprotective role has clearly been identified [12–14]. In the brain, HspB5 is expressed at lower levels but reportedly exerts neuroprotective functions as

Electronic supplementary material The online version of this article (doi:10.1007/s00018-016-2219-9) contains supplementary material, which is available to authorized users.

✉ Nikola Golenhofen
nikola.golenhofen@uni-ulm.de

[1] Institute of Anatomy and Cell Biology, University of Ulm, Albert-Einstein-Allee 11, 89081 Ulm, Germany

well. For example, HspB5-deficient mice show significantly higher infarct sizes after an experimental stroke and more intense inflammation in response to experimental autoimmune encephalomyelitis compared with wild-type mice [15, 16]. In addition, HspB5 and other HspBs are upregulated in glial cells and neurons in several neurodegenerative diseases [17–19], where they are associated with the disease-causing protein aggregates, for example, with β-amyloid in Alzheimer's disease [20, 21], Rosenthal fibers in Alexander disease [22–24], or Lewy bodies in Parkinson's disease [25]. Presumably, HspB5 dampens pathological aggregate formation via its chaperone-like activity. However, the HspB protein family is exceptional among the heat shock proteins with respect to their additional non-chaperone functions. Besides preventing protein denaturation and aggregation, HspB5 has anti-apoptotic and anti-inflammatory properties and interacts with several cytoskeletal proteins, thereby increasing cell viability under cellular stress conditions [16, 26–33]. Therefore, it is likely that HspB5 exerts additional functions in neurons besides its effect on protein aggregation.

HspB5 not only becomes upregulated in response to stress conditions but will also be phosphorylated [34]. HspB5 has three phosphorylation sites at serine 19, 45, and 59 [34, 35]. It is generally believed that phosphorylation increases the cytoprotective effect [36, 37]. Recently, we showed in cultured hippocampal neurons a phosphorylation-dependent recruitment of HspB5 to different cellular compartments, i.e., axons, dendrites, and synapses [38]. These data suggest that neuronal HspB5 functions might also be regulated by phosphorylation.

To obtain hints about possible neuronal functions of HspBs during pathophysiological conditions when they are upregulated, we overexpressed the individual HspBs in cultured hippocampal neurons. We could identify a new function of HspB5 in enhancing the complexity of the dendritic arbor. This stimulating effect was dependent on phosphorylation of HspB5. Furthermore, HspB5 prevented the rarefaction of dendrites upon heat shock. Thus, this study provides a new mechanism of how HspB5 might exert its protective effect in neurons.

Materials and methods

Animal experiments

All animal experiments were performed in compliance with the guidelines for the welfare of experimental animals issued by the Federal Government of Germany, the National Institute of Health, and the Max Planck Society. The described experiments with rat tissue and cultured cells/neurons are approved by the local ethics committee (Ulm University). ID Number: O.103.

Cell culture

Sprague–Dawley rats (Crl:CD, Charles-River Lab. Int. Inc., Wilmington, MA, USA) at 18 or 19 days of gestation were sacrificed by CO_2. After dissection, the embryonal hippocampi were dissociated with 0.25 % trypsin in HBSS (PAA, Pasching, Austria) followed by treatment with 0.01 % DNase I (Life Technologies, Carlsbad, CA, USA). The cell suspension was then passed through a 100-µm sieve, counted, and plated at a density of 15,000–20,000 cells/cm^2 on poly(L)lysine-coated cover slips or petri dishes in DMEM with 10 % FCS. After 3 h, medium was changed to Neurobasal (Life Technologies, Carlsbad, CA, USA) supplemented with B-27 and glutamine. The cells were allowed to grow and to differentiate at 37 °C, 5 % CO_2, 95 % air in a humidified atmosphere.

Lenti-X 293T cells (Clontech, Mountain View, USA) were grown in DMEM with 10 % FCS.

Amplification of HspB cDNAs and cloning into an appropriate expression vector

For overexpression experiments, the coding sequence of rat HspBs was amplified from rat whole brain cDNA with the PCR SuperMix High Fidelity (Life Technologies, Darmstadt, Germany) and the primers shown in Table 1 according to the manufacturer's instructions. The resulting PCR products were cloned into the TOPO TA vector pCR

Table 1 Primer pairs for cloning of rat HspBs

Gene	Primer	Amplicon length (bp)	Annealing (°C)
HspB1	HspB1-BglII-Fw: 5′-GCAGATCTATGACCGAGCGCCGCGTGCCCTTCTCGCTACTGCG	637	63
	HspB1-BamHI-Rev: 5′-CCGGATCCCTACTTGGCTCCAGACTGTTCCGACTCTGGGC		
HspB5	HspB5-BglII-Fw: 5′-GCAGATCTATGGACATAGCCATCCACCACCCCTGGATCCG	544	58
	HspB5-ApaI-Rev: 5′-CCGGGCCCCTACTTCTTAGGGGCTGCAGTGACAGCAG		
HspB6	HspB6-EcoRI-Fw: 5′-CGGAATTCATGGAGATCCGGGTGC	505	65
	HspB6-BamHI-Rev: 5′-GCGGATCCCTACTTGGCAGCAGGT		
HspB8	HspB8-XhoI-Fw: 5′-CTCGAGATGGCTGACGGGCAA-3′	603	58
	HspB8-BamHI-Rev: 5′-GGATCCTTAGGAGCAGGTGACTT-3′		

2.1 (Life Technologies, Darmstadt, Germany) according to the manufacturer's instructions and transformed into *E. coli* DH5α. Subsequently, the respective HspB sequence was excised with EcoRI (Thermo Scientific Inc., St. Leon-Rot, Germany) and cloned into the pLVX-IRES-ZsGreen1 vector (Clontech, Mountain View, USA) using T4 ligase (Thermo Scientific Inc., St. Leon-Rot, Germany). Correct sequence and orientation were controlled by sequencing.

Site-directed mutagenesis

Mutagenesis of HspB5 phosphorylation sites was carried out with the Phusion Site-directed Mutagenesis Kit (Life Technologies, Carlsbad, CA, USA) according to the manufacturer's instructions. The primer pairs, used with 5′ phosphate modification, are listed in Table 2. Briefly, a PCR was carried out with 2 U Phusion Hot Start II Taq polymerase, 0.5 µM of S19A mutagenesis primers, 200 µM dNTPs, and 100 pg of HspB5-containing pCR2.1 TOPO vector as template in Phusion HF reaction buffer. Amplification protocol was 98 °C, 30 s followed by 25 cycles of 98 °C, 10 s, 65 °C, 30 s, 72 °C, 4 min, and a final elongation at 72 °C, 10 min. The PCR products were ligated with T4 ligase and transformed into *E. coli* DH5α. Success of the mutagenesis was assessed by sequencing. Subsequently, the vector containing the S19A mutation was used as template in a PCR with S45A primers, the resulting vector (S19A–S45A) as template for S59A primers. Clones carrying the desired triple-A mutation were then restricted with EcoRI and the insert cloned into pLVX-IRES-ZsGreen 1 as described before.

Production of HspB containing lentivirus

Overexpression of HspB5 in neurons was performed by lentiviral transduction using the Lenti-X^{TM} HT Packaging System (Clontech, Mountain View, USA). The pLVX-IRES-ZsGreen1 empty vector and the various pLVX-IRES-ZsGreen1-HspB vectors were cotransfected with the pMD2 and psPAX2 vectors containing the sequences for the lentiviral packaging proteins into Lenti-X 293T cells (Clontech) according to the manufacturer's instructions. Medium was changed after 24 h, and the viral supernatant was harvested after 48 h. Viruses were stored at −80 °C until further use.

Transduction of hippocampal neurons

Cultured rat hippocampal neurons grown on cover slips were transduced at day in vitro 1 (DIV 1) or at DIV 7 with lentivirus containing either the empty pLVX-IRES-ZsGreen1 vector or the various pLVX-IRES-HspB plasmids. For that purpose, 10-to-100 µl virus supernatant was added to the medium of neuronal cultures. Controls received the same amount of DMEM with 10 % FCS. In cultures to be analyzed at DIV 14, the medium containing the viruses was replaced after 24 h with conditioned medium taken from neuronal cultures that were cultivated in parallel. Neurons were further cultivated and analyzed at DIV 3, DIV 7, or DIV 14 for axon length, synapse density, or dendritic architecture as described in detail below.

Immunocytochemistry

Control and transduced cultured hippocampal neurons were fixed with 4 % formaldehyde in PBS for 20 min at 4 °C. After washing with PBS, cells were permeabilized with 0.1 % Triton-X-100 and 0.1 % sodium citrate in PBS for 5 min at RT, and blocked for unspecific binding with 3 % bovine serum albumin and 1 % normal goat serum in PBS for 30–60 min at RT. The primary antibodies were applied at 4 °C overnight. Primary antibodies and dilutions used are listed in Table 3. After further washing, cells were incubated with either goat anti-rabbit or goat anti-mouse Alexa Fluor 568 or in the case of double labeling with a mixture of goat anti-rabbit Alexa Fluor 568 and goat anti-

Table 2 Primer pairs for site-directed mutagenesis

Site	Primer pair
S19A	S19A-Fw: 5′-TCTTTCCTTTCCACGCCCCAAGCCGCCTC
	S19A-Rev:5′-AGGGACGCCGGATCCAGGGGTGGTGGAT
S45A	S45A-Fw: 5′-ACAGCCACTTCCCTGGCCCCCTTCTACCTTCG
	S45A-Rev: 5′-AGAGAAGAGGTCAGACTCCAACAGGTGCTCTCC
S59A	S59A-Fw: 5′-TTCCTGCGGGCACCTGCCTGGATTGACACTGG
	S59A-Rev: 5′-GGAGGGTGGCCGAAGGTAGAAGGGGGCCAG

Sequences to be mutated are underlined

Table 3 Primary antibodies used for immunocytochemistry

Antibody	Species	Dilution	Distributor
Anti-HspB1	Rabbit	1:200	Stressgen, #SPA-801
Anti-HspB5	Rabbit	1:100	GeneTex, #GTX62094
Anti-HspB6	Mouse	1:200	Acris, #BM2647
Anti-HspB8	Rabbit	1:100	Cell Signaling, #3059
Anti-MAP-2	Mouse	1:500	Millipore, #MAB3418
Anti-MAP-2	Rabbit	1:500	Millipore, #AB5622
Anti-Neurofilament	Mouse	1:2000	Covance, #SMI-312R
Anti-VGLUT1	Rabbit	1:1000	Synaptic Systems, #135 303
Anti-VGAT	Rabbit	1:400	Synaptic Systems, # 131 002

mouse Alexa Fluor 647 (dilutions 1:900, Life Technologies, #A-11036, #A-21124, #A-21235) for 45 min at RT. After final rinsing for 3 × 5 min with PBS, cells were mounted in Mowiol 4.88 (Hoechst, Germany) containing 1 μg/ml DAPI (Applichem, Darmstadt, Germany). Images were acquired on a Zeiss Axioscope2 microscope equipped with an AxioCam MRm camera (Zeiss, Oberkochen, Germany) and analyzed using AxioVision software (Zeiss). Controls were performed by omission of the primary antibodies. In the case of analysis of transduced cultures, only images from transduced neurons showing a clear ZsGreen signal were acquired and analyzed. Cell viability was assessed by DAPI staining. Neurons with pyknotic or apoptotic nuclei were excluded from analysis.

Analysis of axon length

For analysis of axon length, neuronal cultures were transduced at DIV 1 and fixed at DIV 3. Axons were visualized by staining with a pan-axonal neurofilament antibody (see Table 3), which has been developed to label specifically axons and is directed against axon-specific neurofilament subtypes. Images of 16 neurons selected randomly were taken for each experimental condition (blinded) in each experiment, and the length of the axon was measured with AxioVision software. In total, for each condition, 64 neurons were analyzed out of four independent experiments.

Determination of synapse density

For determination of synapse density, neuronal cultures were either transduced at DIV 1 and fixed at DIV 7 or transduced at DIV 7 and analyzed at DIV 14. Images of neurons stained for the presynaptic proteins VGLUT1 (excitatory synapses) or VGAT (inhibitory synapses) in combination with MAP-2 were taken. All VGLUT1- or VGAT-positive dots, respectively, that localized to dendrites and their immediate vicinity were assumed to represent synapses. Synapses of control neurons and neurons transduced with empty-, HspB1-, HspB5-, HspB5, HspB5-AAA-, HspB6-, and HspB8-virus from three to six independent experiments (with at least nine neurons measured per experiment) were used for analysis. For each neuron, VGLUT1- or VGAT-positive puncta, respectively, were counted along a total length of at least 50–100 μm of primary or secondary dendrites with the ImageJ plug-in FindPeaks (GDSC, University of Sussex, UK) and the following settings. For counting of VGLUT1-positive puncta, the background setting was "StdDev above mean," search method "above background," minimum size 5, peak height "relative above background," "minimum above saddle" with a peak parameter of 0.3. For counting of VGAT-positive puncta, the minimum peak height was set to "relative height" and peak parameter changed to 0.25. A region of interest fitting closely around a dendrite was defined prior to automated counting. Synapse density per 10 μm was calculated of each neuron for primary and secondary dendrites separately.

Analysis of the dendritic arbor

For investigation of the dendritic arbor, neuronal cultures were either transduced at DIV 1 and fixed at DIV 7 or transduced at DIV 7 and analyzed at DIV 14. Dendritic complexity was analyzed via Sholl analysis, which quantifies the number of times dendrites from a neuron cross concentric circles of increasing diameters around the neuronal cell body [39]. Dendrites were visualized by MAP-2 staining as described above. The number of dendrites crossing a series of concentric circles at intervals of 15 μm of each neuron was counted manually. For comparison of the effect of various HspBs on dendritic morphology during the second week of differentiation in vitro, Sholl analysis of dendritic arbors was performed of control ($n = 257$), empty-virus ($n = 249$), HspB1-virus ($n = 71$), HspB5-virus ($n = 264$), HspB6-virus ($n = 80$), and HspB8-virus ($n = 110$) transduced neurons. Data were combined from 5 (HspB1- and HspB6-virus), 8 (HspB8-virus), 17 (HspB5-virus), 18 (control), and 19 (empty-virus) independent experiments. For investigation of the importance of phosphorylation of HspB5 neurons of control, empty-virus (empty vector), HspB5-virus, and HspB5-AAA-virus transduced neurons were analyzed in separate sets of experiments. For each condition, a total of 60 neurons from six independent experiments were analyzed. For analysis of the dendritic arbor after 1 week in culture (transduction at DIV 1 and analysis at DIV 7) for each condition (control, empty-, HspB1, HspB5-, HspB5-AAA, HspB6-, and HspB8-virus), a total number of 75 neurons from four independent experiments were analyzed.

All samples were blinded before analysis, and neurons were selected randomly.

Heat shock experiments

For these experiments, neurons were transduced at DIV 7 with empty-, HspB5, and HspB5-AAA-virus. Heat shock was carried out at DIV 14 in a temperature-controlled water bath at 43 °C for 30 min. After that, neurons were placed back into the incubator for further 2 days prior to fixation and analysis (DIV16). Analysis of the dendritic arbor was performed as described above. Unstressed neurons transduced with empty-virus were used for comparison. For each condition, a total of 30 neurons from three independent experiments were analyzed.

Statistics

Data are presented as mean ± standard error of the mean. As our data were not normally distributed, the non-parametric Mann–Whitney U test was used for statistical analysis. Statistical significance was assumed for $p < 0.05$.

Results

Transduction of cultured rat hippocampal neurons with HspB containing lentivirus

To investigate neuronal functions of HspBs, we overexpressed them in cultured rat hippocampal neurons by a lentiviral expression system. From the ten HspB family members, four (HspB1, HspB5, HspB6, and HspB8) are known to be expressed in this cellular system [11] and, thus, were chosen for overexpression experiments. The coding sequences of HspB1 (Hsp27), HspB5 (αB-crystallin), HspB6 (Hsp20), and HspB8 (Hsp22) were amplified from rat whole brain cDNA and cloned into the bicistronic vector pLVX-IRES-ZsGreen1. Lentiviruses containing either the empty vector or the vector with the respective HspB (in the following called "empty-virus" and "HspB-virus") were produced. Depending on the objective of investigation, different time courses of transduction and analysis were needed. For analysis of axonal growth, hippocampal neurons were transduced after 1 day in culture (day in vitro 1, DIV 1) and used for measurements at DIV 3. For investigation of the dendritic arbor and synapses, neurons were either transduced at DIV 1 and analyzed at DIV 7 or transduced at DIV 7 and analyzed at DIV 14. Overexpression of the respective proteins in neuronal cultures was controlled in all cases by immunocytochemistry. Figure 1 shows cultured hippocampal neurons infected with all types of viruses at DIV 7 and immunolabeled for microtubule-associated-protein-2 (MAP-2) and the respective HspBs at DIV 14. Figure 1a shows double labeling for MAP-2 and HspB1 of neurons transduced with empty- and HspB1-virus demonstrating successful overexpression. Transduced neurons could be identified by ZsGreen1 fluorescence. MAP-2 positive cells represented neurons. Control neurons (data not shown) as well as neurons transduced with empty-virus showed a very faint immunosignal for HspB1, which was only visible after longer exposure times, whereas neurons transduced with HspB1-virus were characterized by prominent immunolabeling for HspB1 of the whole neuron, including the perikaryon and neurites. Thus, transduction of neurons resulted in overexpression of HspB1. Figure 1b–d show experiments performed in parallel demonstrating neuronal overexpression of HspB5, HspB6, and HspB8 by lentiviral transduction.

Overexpression of HspBs did not affect axon length

HspB overexpressing neurons were analyzed for potential alterations of their morphology, i.e., axon length, dendritic arborization, and synapse density. For the measurement of axon length, neurons were transduced at DIV 1 and stained 2 days later with an antibody against MAP-2 to visualize dendrites and with an antibody against axon-specific neurofilament to identify the axon. Later time points were not suitable for investigation because of the difficulty to trace the axon within the complex neuronal network. In addition, according to the stages defined by Dotti and Banker [40], axonal outgrowth starts at DIV 1.5, whereas dendritic outgrowth takes place later around DIV 4. Figure 2a shows representative images of control and transduced neurons at the time point of analysis. The antibody against axon-specific neurofilament stained mainly one neurite that was considered to represent the axon (stained in red). Untransduced neurons (ctrl) displayed an average axon length of 239.1 ± 8.4 µm, which was not significantly altered by overexpression of the empty vector, HspB1, HspB5, HspB6, or HspB8 (Fig. 2b).

HspB5 and HspB6 increased dendritic branching

The relevance of HspBs in neuronal process elaboration was investigated by overexpression of HspBs and performing Sholl analysis, which is a measure for the complexity of the dendritic tree by assessing the number of crossing points of dendrites with concentric circles of increasing diameters around the cell body. Since, in hippocampal cultures, dendritic branching and the complexity of the dendritic arbor develop mainly in the second week, we first transduced neurons at DIV 7 with empty-virus and the various HspB-viruses, fixed them at DIV 14, and identified dendrites by immunostaining for MAP-2. Figure 3a shows a representative MAP-2 stained neuron transduced with empty-virus. In addition, the concentric circles for Sholl analysis are displayed in the figure, and exemplarily, the intersections of dendrites with the circle at a distance of 60 µm from the soma are indicated by small circles. Successful transduction of neurons was verified by the ZsGreen signal (Fig. 1) of all neurons analyzed. A systematic analysis revealed that overexpression of HspB5 resulted in increased dendritic branching, especially of the secondary and higher order dendrites demonstrated by statistically significant more intersections at 30–165 µm from the cell body compared to neurons transduced with empty-virus (Fig. 3b). Dendritic branching was also increased by HspB6, but to a lesser extent and only between distances of 75 and 165 µm from the soma. Interestingly, HspB6 led to a smaller amount of primary

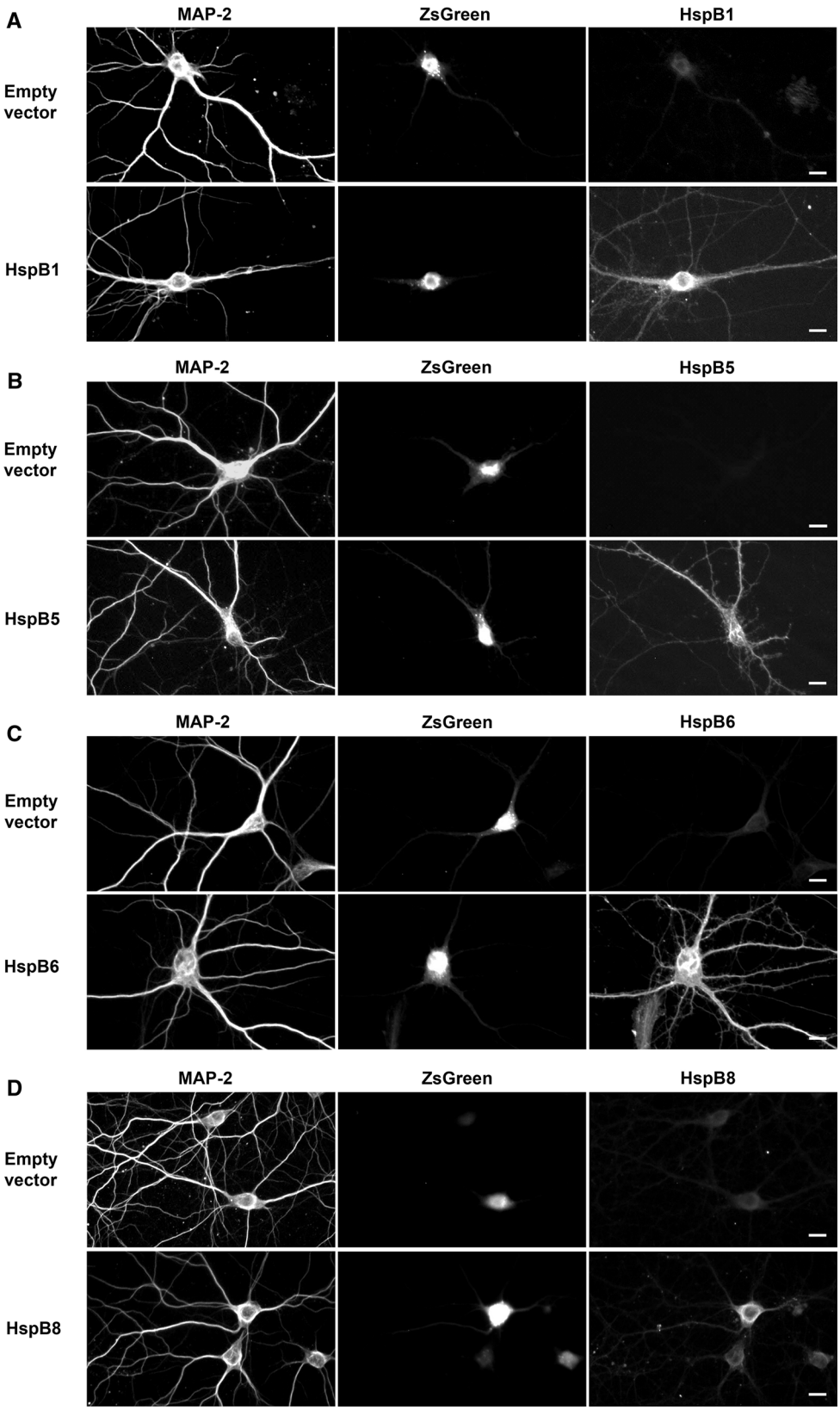

Fig. 1 Overexpression of HspBs in cultured rat hippocampal neurons. Immunocytochemical staining of representative neurons transduced with empty-virus (empty vector) and **a** HspB1-virus, **b** HspB5-virus, **c** HspB6-virus, and **d** HspB8-virus at DIV 7 and fixed and stained at DIV 14. The *first column* shows staining for the dendritic marker MAP-2 allowing identification of neurons, the *second column* shows ZsGreen fluorescence indicating transduction, and the *third column* shows the staining against the respective HspB. In empty-virus transduced neurons, a weak or no immunosignal for all HspBs in the perikaryon could be observed. In neurons transduced with HspB-virus, the staining intensity was increased and HspBs localized diffusely in the whole neuron, including neuronal processes indicating successful overexpression. Images of neurons transduced with empty-virus and HspB-virus were taken with the same exposure time. *Bar* 10 μm

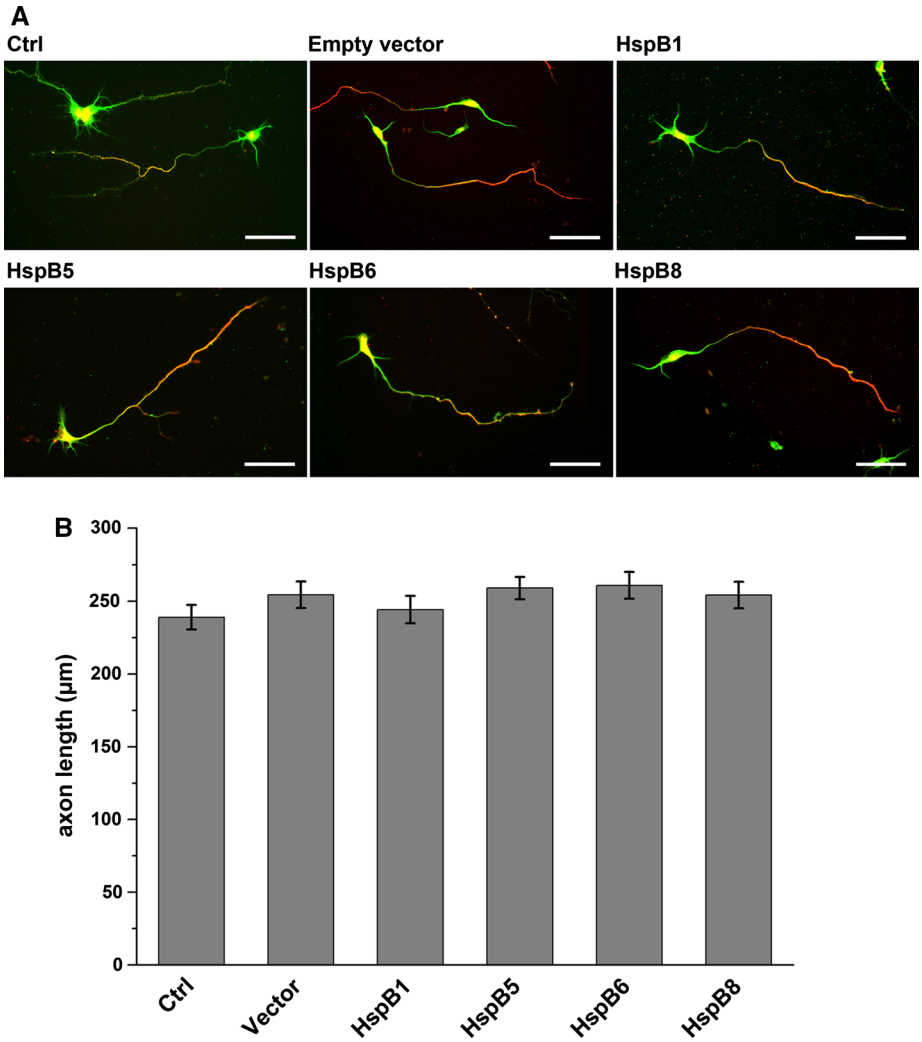

Fig. 2 Measurement of axon length in HspB overexpressing cultured hippocampal neurons. **a** Representative images of a control neuron and neurons transduced with empty-virus (empty vector), HspB1-, HspB5, HspB6-, and HspB8-virus at DIV 1 and analyzed at DIV 3. Neurons were labelled with antibodies against MAP-2 (dendrites, *green*) and axon-specific neurofilament (axon, *red*). *Bar* 50 µm. **b** Measurement of axon length of control (Ctrl), empty-virus (vector), HspB1-virus, HspB5-virus, HspB6-virus, and HspB8-virus transduced neurons. No significant differences between the various cultures could be observed. For each condition, a total of 64 neurons from four independent experiments were analyzed

dendrites reflected by fewer crossing points of dendrites with the circle 15 µm away from the cell body. HspB1 and HspB8 overexpression did not significantly affect the complexity of the dendritic tree.

Since the effect on dendritic complexity was strongest in HspB5 overexpressing neurons, we focused on HspB5 in the following experiments.

The effect of HspB5 on the dendritic arbor was phosphorylation dependent

The properties of HspB5 are known to be regulated by phosphorylation and phosphorylation of HspB5 was shown to be important for its dendritic and synaptic localization previously [38]. For this reason, we addressed the question if phosphorylation of HspB5 is required for its stimulating effect on dendritic branching. We generated a non-phosphorylatable HspB5 mutant by replacing serine 19, 45, and 59 with alanine ("HspB5-AAA") using site-directed mutagenesis, followed by production of the respective lentivirus. Hippocampal neurons were transduced with empty-virus, HspB5-virus, and HspB5-AAA-virus, and dendritic branching was analyzed by Sholl analysis as described in the previous paragraph. Overexpression of HspB5-AAA was confirmed by immunocytochemical staining with the anti-HspB5 antibody (Fig. 4a). Figure 4b shows representative tracing images of a neuron transduced with empty-virus, HspB5-virus, and HspB5-AAA-virus. Figure 4c displays the results of the Sholl-analysis. HspB5 overexpression had a prominent effect on arborization of the dendritic tree, whereas overexpression of HspB5-AAA did not result in increased dendritic branching. Thus, phosphorylation of HspB5 was required for the dendritic function of HspB5.

In addition, we investigated the effects of HspBs on dendritic arborization during the first week of differentiation in culture (transduction at DIV 1 and Sholl-analysis at DIV 7). At the end of the first week, the dendritic arbor of control neurons consisted mainly of primary dendrites with

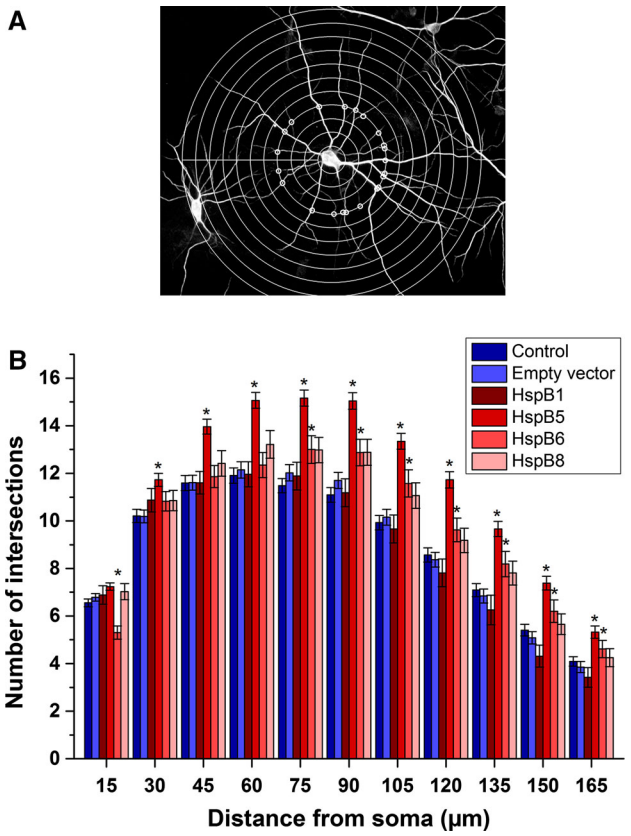

Fig. 3 Sholl analysis of HspB overexpressing cultured hippocampal neurons. **a** Representative neuron transduced with empty-virus at DIV 7 stained for MAP-2 at DIV 14 illustrating the method of Sholl analysis. *Concentric circles* were drawn at 15 µm intervals around the cell soma and crossing points of dendrites with each *circle* counted. The intersections of dendrites with the *concentric circle* at a distance of 60 µm from the cell body are marked exemplarily by *small circles*. **b** Sholl analysis of dendritic arbors of control ($n = 257$), empty-virus ($n = 249$), HspB1-virus ($n = 71$), HspB5-virus ($n = 264$), HspB6-virus ($n = 80$), and HspB8-virus ($n = 110$) transduced neurons. Note significantly increased number of intersections for HspB5-transduced neurons in the range of 30–165 µm and for HspB6-transduced neurons in the range of 75–165 µm from the cell body compared with empty-virus transduced neurons. $^*p < 0.05$ versus empty-virus transduced neurons

a few branches and a few secondary and tertiary dendrites. Figure 5 shows the results of Sholl analysis of control neurons and neurons transduced with empty-, HspB5-, and HspB5-AAA-virus. At this early time points, only subtle changes could be observed. At distances of 15–60 µm from the soma, HspB5 had no effect on dendritic arborization. At distances further away, neurons transduced with empty-virus showed strangely a slight but significant reduction in the number of intersections, and thus, HspB5 overexpressing neurons showed a slight significant increase in dendritic arborization compared to neurons transduced with empty vector but not to controls. Hence, one might conclude that during early stages in contrast to late stages of dendritic development, HspB5 has no major relevant impact on dendritic branching. Interestingly, HspB5-AAA expressing neurons displayed the lowest number of intersections differing between 15 and 90 µm significantly from HspB5 expressing neurons. This underlines the importance of phosphorylation of HspB5 for its dendritic function, as described above.

For the sake of completeness, we also investigated the effects of HspB1, HspB6, and HspB8 on dendritic branching at this early time point, but could not observe relevant effects of these HspBs on the dendritic arbor (online resource 1).

HspBs did not affect synapse density

Next, we investigated if HspB5 or other HspBs might influence synapse density. First, we transduced hippocampal neurons at DIV 7 with empty-virus, HspB5-virus, and HspB5-AAA-virus, and stained at DIV 14 for synapses using antibodies against the vesicular glutamate transporter 1 (VGLUT1) and the vesicular GABA-transporter (VGAT), respectively. VGLUT1- and VGAT-positive puncta were assumed to represent excitatory and inhibitory synapses, respectively. Additional staining for MAP-2 allowed assigning the VGLUT1- or VGAT-positive puncta to different categories of dendrites, i.e., primary or secondary dendrites. Figure 6 shows representative parts of dendrites of hippocampal neurons transduced with empty-virus labeled for MAP-2 and VGLUT1 or VGAT (Fig. 6a). Synaptic puncta of untransduced and transduced neurons (identified by ZsGreen fluorescence) were counted. Control neurons were characterized by 6.2 ± 0.24/10-µm VGLUT1-positive puncta along primary and 4.4 ± 0.19/10-µm puncta along secondary dendrites. This number was not significantly altered in neurons transduced with any virus. The quantity of VGAT-positive puncta was in general lower, namely, 3.1 ± 0.15/10 µm along primary and 2.0 ± 0.11/10 µm along secondary dendrites of control neurons. Transduction of neurons with the various types of viruses led to very little changes, which reached the level of significance only in the case of transduction with HspB5-virus for VGAT-positive puncta at secondary dendrites (1.8 ± 0.1/10 µm). Even though this effect was significant, it can be assumed that it is not of functional relevance. In a second separate experimental series, we investigated potential effects of HspB1, HspB6, and HspB8 on synapse density. The experimental protocol was identical to that described above for HspB5. Figure 7 shows that these three HspBs did not alter synapse density significantly. We also investigated potential effects of HspBs at an earlier time point (transduction at DIV 1 and analysis at DIV 7), but could also see no significant changes (online resource 2). At this early time point, nearly no VGAT-positive puncta could be identified and, thus, could not be analyzed. Taken together, these data suggest that synapse density, either of excitatory or of inhibitory

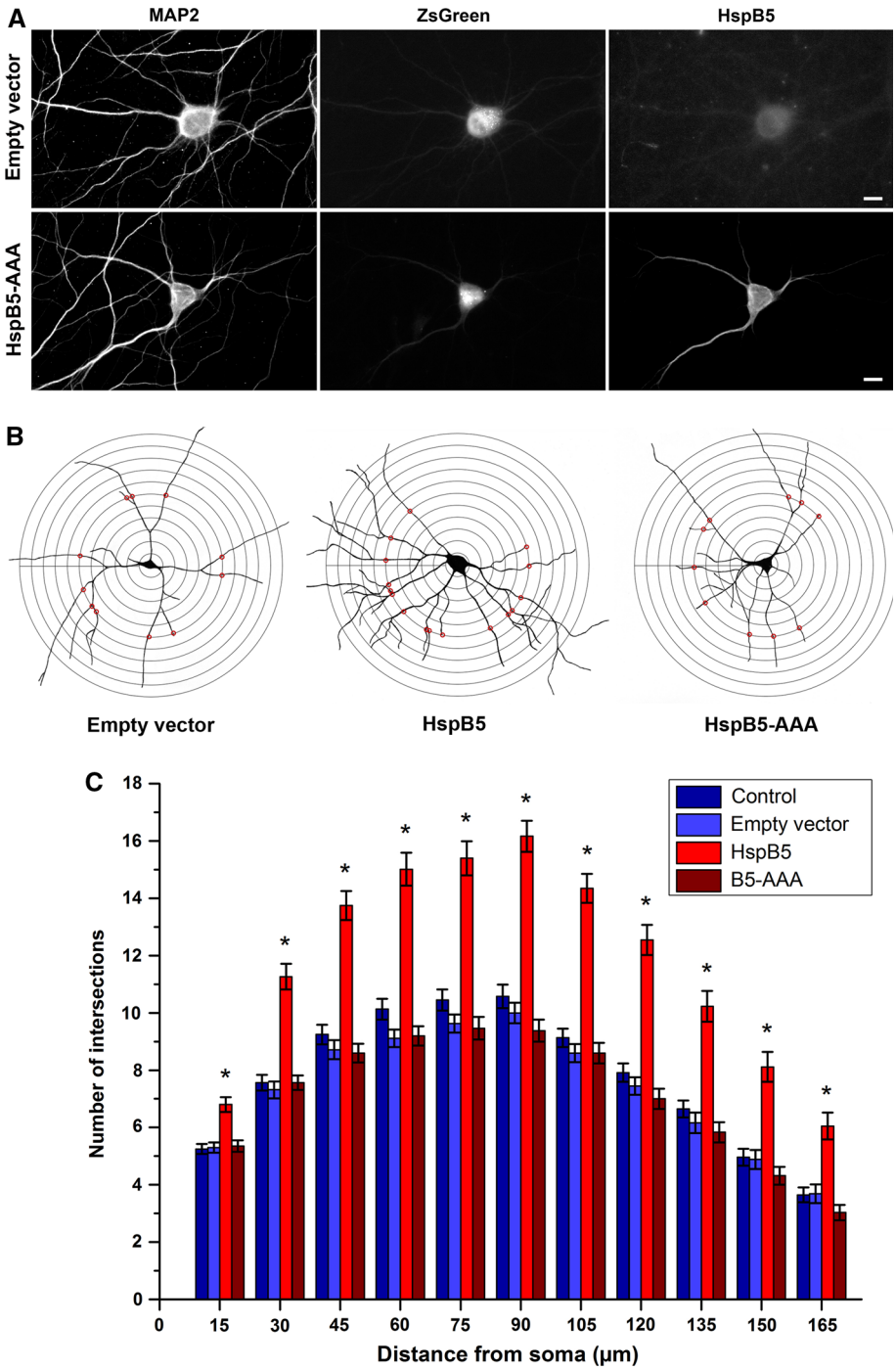

Fig. 4 Sholl analysis of cultured hippocampal neurons overexpressing non-phosphorylatable HspB5-AAA. **a** Immunocytochemical staining for MAP-2 and HspB5 of representative neurons transduced with empty-virus (empty vector) and HspB5-AAA-virus. MAP-2 positive cells represent neurons, the ZsGreen fluorescence indicates successful transduction, and the prominent HspB5 immunoreactivity in HspB5-AAA-virus transduced cells shows overexpression of HspB5-AAA. Images of empty-virus and HspB5-AAA virus transduced cells were taken with the same exposure time. *Bar* 10 µm. **b** Representative drawings of neurons transduced at DIV 7 with empty-virus, HspB5-virus, and HspB5-AAA-virus with immunocytochemical staining for MAP-2 at DIV 14. Intersections of dendrites with the Sholl circle at a distance of 90 µm from the soma are indicated by *small red circles*. **c** Sholl analysis of dendritic arbors of control, empty-virus (empty vector), HspB5-virus, and HspB5-AAA-virus transduced neurons. For each condition, a total of 60 neurons from six independent experiments were analyzed. Note significant increase in dendritic complexity only in HspB5- and not in HspB5-AAA-transduced neurons. $^{*}p < 0.05$ versus empty-virus transduced neurons

synapses, is not significantly influenced by any HspB or the effect was too small to be of functional relevance.

HspB5 protected the dendritic arbor from heat shock-induced rarefaction

The observed effect of HspB5 on the dendritic arbor described above will be functionally most important in vivo under circumstances when HspB5 is upregulated and phosphorylated. This is the case during neuronal stress conditions or in several disease states (see "Discussion"). Several pathophysiological events are characterized by a rarefaction of the dendritic complexity resulting in dysfunction of neurons. To investigate if upregulated and phosphorylated HspB5 might counteract the rarefaction of the dendritic arbor under such conditions, we tried to simulate such a situation in our experimental system.

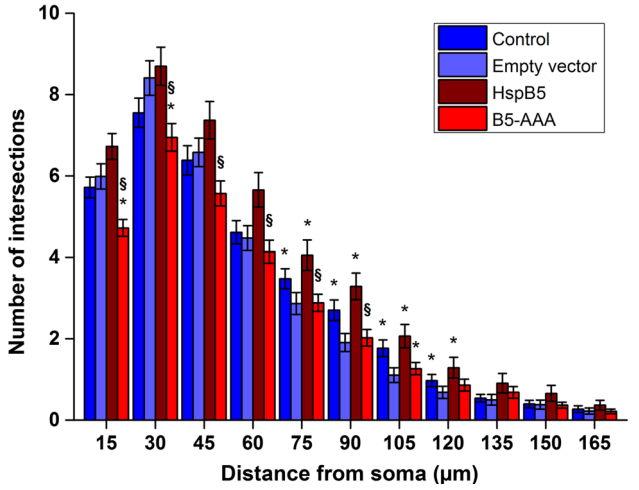

Fig. 5 Sholl analysis of cultured hippocampal neurons overexpressing HspB5 and HspB5-AAA after 1 week of differentiation. Sholl analysis of dendritic arbors at DIV 7 of control neurons and neurons transduced at DIV 1 with empty-, HspB5, and HspB5-AAA-virus. Note significant differences between HspB5 and HspB5-AAA expressing neurons suggesting the importance of phosphorylation of HspB5 for its dendritic function, $n = 75$ (75 neurons from three independent experiments), $^{*}p < 0.05$ versus empty-vector, $^{\S}p < 0.05$ versus HspB5

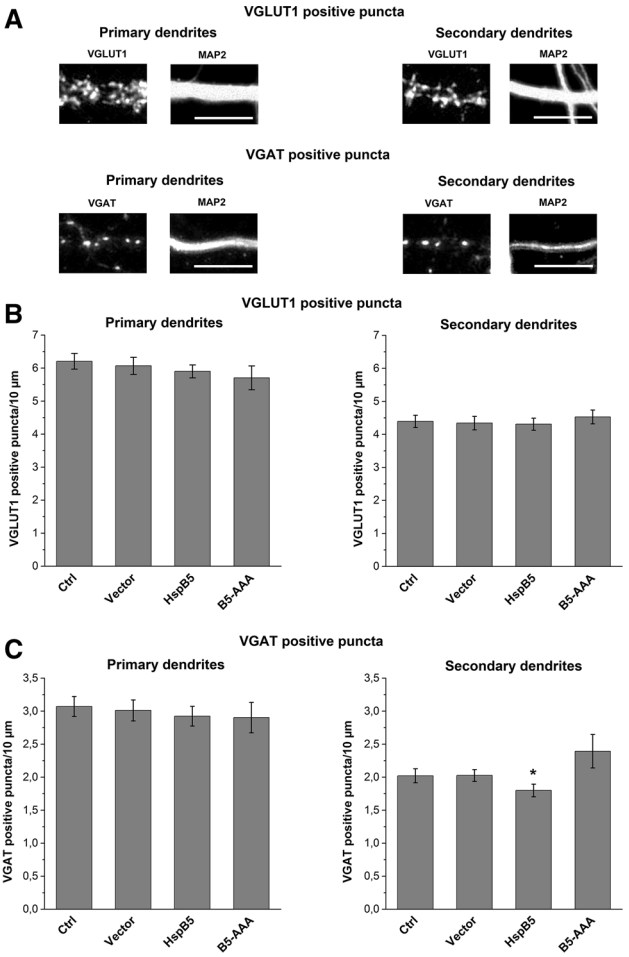

Fig. 6 Effect of overexpression of HspB5 and non-phosphorylatable HspB5-AAA on synapse density. **a** Representative parts of primary and secondary dendrites of empty-virus transduced neurons immunolabelled with VGAT or VGLUT1 and MAP-2. Neurons were transduced at DIV7 and analyzed at DIV 14. *Bar* 10 µm. **b** Measurement of VGLUT1-positive puncta on primary (*left column*) and secondary (*right column*) dendrites of control neurons (Ctrl, $n = 60$) and neurons transduced with empty-virus (vector, $n = 55$), HspB5-virus (HspB5, $n = 57$), and HspB5-AAA-virus (B5-AAA, $n = 27$). **c** Measurement of VGAT-positive puncta on primary (*left column*) and secondary (*right column*) dendrites of control neurons (Ctrl, $n = 55$) and neurons transduced with empty-virus (vector, $n = 58$), HspB5-virus (HspB5, $n = 54$), and HspB5-AAA-virus (B5-AAA, $n = 27$). $^{*}p < 0.05$ versus empty-virus transduced neurons

For that purpose, we stressed hippocampal neurons by exposure to heat shock and analyzed the dendritic tree by Sholl analysis afterward. In pilot tests, we identified a suitable strength of stress, which led to significant reduction of dendritic complexity but not to cell death. Cell viability was assessed by visual inspection of neuronal morphology and intact cell nuclei stained with DAPI. Next, neurons transduced at DIV 7 with empty-, HspB5, and HspB5-AAA-virus were stressed at DIV 14 for 30 min at 43 °C and compared 2 days later (DIV 16) with unstressed neurons transduced with empty-virus. Unstressed neurons transduced with empty-virus exhibited a maximum number of about 16 intersections of dendrites with Sholl circles (Fig. 8). This number was higher compared with the previous experiments (see Figs. 3, 4), which is most likely due to the later time point of analysis, i.e., DIV 16 compared with DIV 14. Heat shock led to a significant reduction of dendritic arborization (20–30 % reduction of the number of intersections at distances from 15 to 120 µm from the soma) in neurons transduced with empty-virus (Fig. 8, blue and green columns). Transduction with HspB5-virus counteracted this process reaching significant levels at Sholl circles 15–105 µm from the soma. HspB5-AAA had also a positive effect on the dendritic tree but not to the same extent as HspB5 wild-type (significant differences at 45 µm and from 75 to 105 µm from soma). Thus, HspB5 promotes maintenance of dendrites during heat shock. Non-phosphorylatable HspB5 preserves the dendritic architecture as well, but to a lesser extent than wild-type HspB5. These data suggest that phosphorylation of HspB5 is not absolutely necessary but intensifies the protective effect of HspB5 on the dendritic arbor.

Discussion

The dendritic arbor is crucial for building functional neuronal networks and normal communication between neurons. Receiving, integrating, and processing of inputs

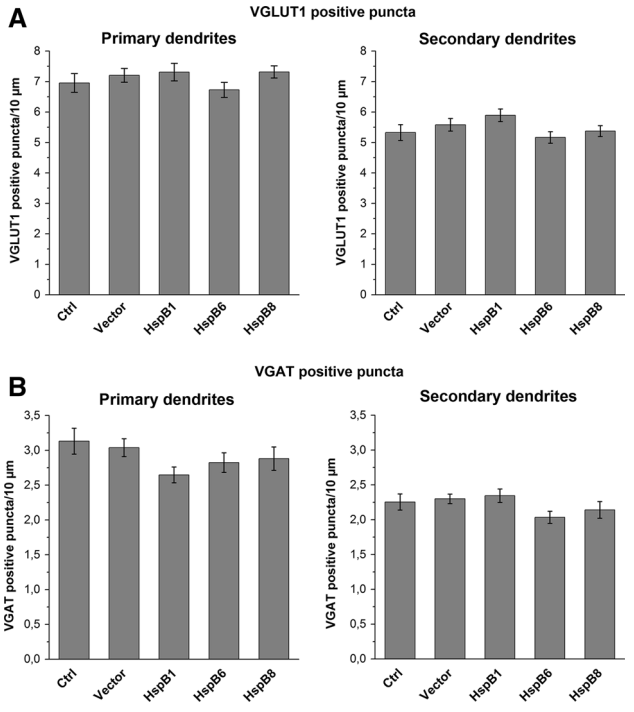

Fig. 7 Effect of overexpression of HspB1, HspB6, and HspB8 on synapse density. Neurons were transduced at DIV7 with the respective viruses and analyzed at DIV 14. Measurement of **a** VGLUT1-positive puncta and **b** VGAT-positive puncta on primary (*left column*) and secondary (*right column*) dendrites of control neurons (Ctrl) and neurons transduced with empty-virus (vector), HspB1-virus, HspB6-virus, and HspB8-virus. No significant differences could be observed. For each condition, 30 neurons from three independent experiments were analyzed

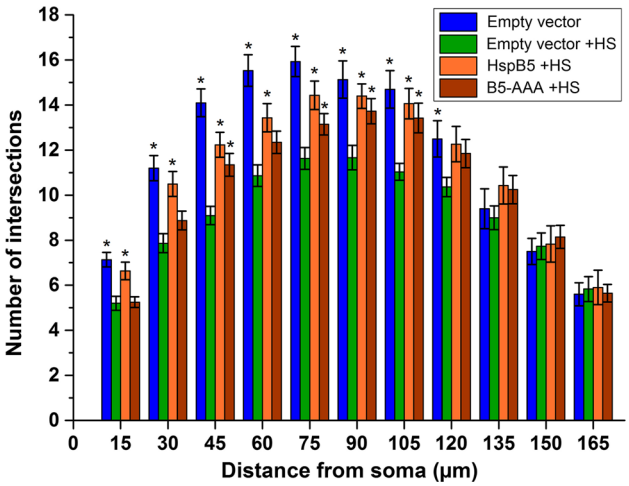

Fig. 8 Sholl analysis of heat-shocked hippocampal neurons overexpressing HspB5 or HspB5-AAA. Sholl analysis of dendritic arbors of empty-virus (empty vector), HspB5-virus, and HspB5-AAA-virus transduced neurons (at DIV 7) exposed to heat shock (30 min 43 °C) at DIV 14 compared with unstressed empty-virus transduced neurons. The dendritic arbor was analyzed after 2 days of recovery at DIV 16. Note significant decrease in dendritic complexity after heat shock in empty-virus transduced neurons (*green columns*) compared with unstressed cells (*blue columns*) at a distance of 15–120 µm from cell soma. Transduction with HspB5-virus (*orange columns*) or HspB5-AAA (*brown columns*) counteracted this process indicating that HspB5 promotes maintenance of dendrites during heat shock. For each condition, a total of 30 neurons from three independent experiments were analyzed. *$p < 0.05$ versus empty-virus transduced heat-shocked neurons

all depend on the complexity of the dendritic arbor. Altered dendritic morphogenesis will lead to neuronal dysfunction resulting in various neurological disorders and diseases. In this study, we describe a new function of HspB5 in increasing dendritic branching and protection of the dendritic integrity upon heat shock.

HspBs and regulation of neuronal complexity

Several members of the HspB family have been shown to be expressed in the brain. Interestingly, our data show a function of HspB5 on the dendritic arbor, which was only shared by HspB6 to a lesser extent but not by HspB1 and HspB8. Although HspBs interact with each other fulfilling their common chaperone-like function, there is increasing evidence that single family members display specific additional functions. For example, HspB5 also displays anti-apoptotic functions and anti-inflammatory properties, and interacts with cytoskeletal proteins [41–43].

Whereas HspB5 has been studied extensively in glial cells, less attention has been drawn to neuronally derived HspB5 [44–48]. In early studies, HspB5 was not detected in neurons in the brain under normal conditions applying immunohistochemical methods. However, neuronal expression of HspB5 was found in the so-called ballooned neurons and at certain pathophysiological conditions [49–53]. Moreover, in cultured hippocampal neurons, HspB5 was recruited by phosphorylation to different subcellular compartments, i.e., axons, dendrites and synapses [38]. These data suggest that HspB5 is expressed at very low levels under control conditions and may exert its function after upregulation and phosphorylation at cellular stress conditions. The overexpression experiments performed in this study were intended to simulate the pathophysiological situation with upregulated HspB5. However, one has to consider that the expression levels of HspBs in the overexpression experiments can be assumed to be higher compared with the levels in stressed neurons. We have chosen two different experimental protocols to assess the degree of dendritic arborization and synapse density. First, we transduced neurons at DIV 1 and analyzed them at DIV 7, and second, we performed transduction at DIV 7 and analysis at DIV 14. In dissociated cultured hippocampal neurons, primary dendrites extend from the cell body mainly during the first week in culture, whereas maturation of the dendritic arbor with elongation of the primary

dendrites, pruning of the branches in close proximity to the soma and increasing branch density more distant to the soma, begins at DIV 7. Thus, further branching and the formation of synapses take place mainly during the second week in vitro [40, 54, 55]. Our data show that elevated levels of HspB5 increased the complexity of the dendritic arbor during the second week of differentiation but did not affect axon growth and synapse density. Thus, one might hypothesize that upon upregulation during neuronal stress conditions HspB5 plays an important role in maintaining the dendritic architecture. Dendritic branching was significantly increased by HspB5 at distances of 30–165 µm from the cell body where the dendritic tree consists predominantly of secondary and tertiary dendrites. The number of primary dendrites was less affected, which was probably due to the time point of transfection, i.e., DIV 7, when primary dendrites are already well developed. In addition, in more immature neurons analyzed at DIV 7, overexpression of HspB5 did not lead to such profound changes in dendritic complexity. It is not uncommon that neurons of different developmental stages react differently to the overexpression of proteins influencing dendritic branching [54, 56]. Thus, our data suggest that HspB5 exerts its effect during the maturation of the dendritic tree, maybe through stabilizing otherwise pruned branches.

HspB6 also showed a significant effect on dendritic branching during the second week of differentiation, although to a lesser extent than HspB5. Interestingly, HspB6 overexpression led to a reduced number of primary dendrites, while increasing higher order dendrite number. HspB6 was found to be transiently upregulated in the apical dendrites of the stratum radiatum in CA1 in gerbil hippocampus after ischemia, peaking 48 h after the insult [57]. This could point to a role of HspB6 in protection the dendritic arbor during ischemia.

HspB8 overexpression resulted in our study in a trend to increased dendritic branching, which did not reach the level of significance in 2-week-old neurons. However, earlier studies have shown that mutations in the α-crystallin domain of HspB8 cause motoneuron specific reduction of neurite number and length [58]. One might, therefore, speculate that HspB8 plays a more important role in motoneurons of the peripheral nervous system (PNS). Furthermore, in the PNS, an effect of HspB1 on axonal growth of sensory neurons has been reported [59], whereas no effects on neuronal morphology could be detected in 2-week-old hippocampal neurons in this study. Thus, the different members of the HspB family may display cell-type specific functions.

From the fact that HspB5 and HspB6 increased dendritic branching and, thus, the number of secondary and tertiary dendrites, one can conclude that total dendritic length will be elevated as well. Thus, in HspB5 and HspB6 overexpressing neurons, the total number of synapses per neuron is estimated to be much higher compared with control even though synapse density was not altered.

Phosphorylation of HspB5

HspB5 has possible phosphorylation sites at Ser-19, Ser-45, and Ser-59 and is phosphorylated in many different cell types in response to stress [34, 35, 60, 61]. Phosphorylation seems to be important for the development of stress tolerance. For example, mimicking phosphorylation of HspB5 protects cardiac myocytes from apoptosis [36] or astrocytes from staurosporine-induced cell death [37]. Several kinase cascades seem to be associated with phosphorylation of HspB5. So far, it seems to be clear that HspB5 is phosphorylated at Ser-59 via the p38-MAPK pathway [34, 62–64], whereas p44 MAP kinase might phosphorylate serine 45 [34]. It is not yet known, which kinase is responsible for the phosphorylation of Ser-19. In vitro, additionally, cAMP-dependent phosphorylation of HspB5 has been described [34, 62, 65].

Our data indicate that the identified dendritic function of HspB5 is dependent on phosphorylation, since a non-phosphorylatable mutant (all three serines replaced by alanine) did not increase dendritic branching in mature (DIV14) or in immature (DIV7) neurons.

However, dendrite maintenance after heat shock-induced neuronal stress was ensured by wild-type HspB5 as well as by the non-phosphorylatable mutant even though to a lower extent. Furthermore, the subcellular localization of phosphorylated HspB5 within dendrites in contrast to the localization of unphosphorylated HspB5 in the perikaryon [38] substantiates the importance of phosphorylation of HspB5 for its function on the dendritic arbor. In that previous study [38], we could show in cultured hippocampal neurons that unphosphorylated HspB5 localized primarily to the perikaryon, whereas phoshpoHspB5 was found in axons and dendrites. Interestingly, the staining pattern within the dendrites differed depending on which of the three posphospecific antibodies was used (against serine 19, 45, and 59). We could observe staining of the dendritic plasma membrane, the filaments within the center of the dendrites, or labeling of spines. Thus, one might speculate that phosphorylation of HspB5 leads to translocation of HspB5 to dendritic structures, thereby interacting with yet unknown molecular targets resulting in regulation of dendritic complexity. Further experiments will be needed to identify, which phosphorylation sites might be responsible for this process.

Functional implications of HspB5 under pathophysiological conditions

It is generally believed that HspB5 fulfils its major function under pathophysiological situations where it is upregulated and phosphorylated. Especially in the brain, HspB5 is expressed at very low levels during normal conditions and also during embryonal development [11]. Thus, it is unlikely that HspB5 contributes significantly to dendrite development during the embryonal period. Rather, the data of this study point to an important function of HspB5 in neurons after upregulation and phosphorylation. HspB5 is upregulated in vivo in many neurodegenerative diseases, such as Alzheimer's or Parkinson's disease [20, 21, 66, 67]. The role of HspB5 in neurodegenerative diseases has not been unraveled. Most studies focus on the inhibitory effect of HspB5 on pathological protein aggregation mediated by its chaperone-activity. HspB5 inhibits amyloid-β fibril formation [68–70] as well as α-synuclein fibril formation [71–73], important pathological processes in the pathogenesis of Alzheimer's and Parkinson's disease, respectively. However, the molecular mechanisms of the toxic effect of these pathological protein aggregates, such as amyloid-β, are not understood. Key changes observed in such neurodegenerative diseases are alterations of the dendritic architecture, spine density, and synaptic loss [74–77]. Reduced dendritic arbors characterized by lower total dendritic length and diminished branching were reported in hippocampal neurons in Alzheimer patients [78, 79]. Our data point to a possible new function of HspB5 in hippocampal neurons. Its stimulating effect on dendritic branching observed at control conditions in this study might become relevant during pathological situations counteracting the dendritic rarefaction during neuronal stress conditions or neurological diseases. Indeed, our results show that overexpression of HspB5 can protect the dendritic arbor from one kind of neuronal stress, i.e., heat shock-induced rarefaction. Thus, HspB5 seems to play a role in long-term maintenance of dendrites and neuronal connectivity, which is crucial for correct functioning of the brain. If this dendritic function of HspB5 proves to be an important endogenous protective process, it will be an interesting point for future studies and would open up new prospects for the treatment of neurodegenerative diseases.

Acknowledgments We thank Bianca Mekle, Stephanie Sues and Diana Reinhardt for their excellent technical assistance.

References

1. Kitagawa K, Matsumoto M, Tagaya M et al (1990) 'Ischemic tolerance' phenomenon found in the brain. Brain Res 528:21–24
2. Obrenovitch TP (2008) Molecular physiology of preconditioning-induced brain tolerance to ischemia. Physiol Rev 88:211–247
3. Moncayo J, de Freitas GR, Bogousslavsky J, Altieri M, van Melle G (2000) Do transient ischemic attacks have a neuroprotective effect? Neurology 54:2089–2094
4. Kitagawa K (2012) Ischemic tolerance in the brain: endogenous adaptive machinery against ischemic stress. J Neurosci Res 90:1043–1054
5. Ritossa FM (1962) A new puffing pattern induced by a temperature shock and DNP in *Drosophila*. Experientia 18:571–573
6. Vos MJ, Hageman J, Carra S, Kampinga HH (2008) Structural and functional diversities between members of the human HSPB, HSPH, HSPA, and DNAJ chaperone families. Biochemistry 47:7001–7011
7. Welch WJ (1992) Mammalian stress response: cell physiology, structure/function of stress proteins, and implications for medicine and disease. Physiol Rev 72:1063–1081
8. Kappe G, Franck E, Verschuure P et al (2003) The human genome encodes 10 alpha-crystallin-related small heat shock proteins: HspB1-10. Cell Stress Chaperones 8:53–61
9. Kappe G, Boelens WC, de Jong WW (2010) Why proteins without an alpha-crystallin domain should not be included in the human small heat shock protein family HSPB. Cell Stress Chaperones 15:457–461
10. Bellyei S, Szigeti A, Pozsgai E et al (2007) Preventing apoptotic cell death by a novel small heat shock protein. Eur J Cell Biol 86:161–171
11. Kirbach BB, Golenhofen N (2011) Differential expression and induction of small heat shock proteins in rat brain and cultured hippocampal neurons. J Neurosci Res 89:162–175
12. Ray PS, Martin JL, Swanson EA et al (2001) Transgene overexpression of αB crystallin confers simultaneous protection against cardiomyocyte apoptosis and necrosis during myocardial ischemia and reperfusion. Faseb J 15:393–402
13. Golenhofen N, Redel A, Wawrousek EF, Drenckhahn D (2006) Ischemia-induced increase of stiffness of alphaB-crystallin/HSPB2-deficient myocardium. Pflugers Arch 451:518–525
14. Morrison LE, Whittaker RJ, Klepper RE, Wawrousek EF, Glembotski CC (2004) Roles for alphaB-crystallin and HSPB2 in protecting the myocardium from ischemia-reperfusion-induced damage in a KO mouse model. Am J Physiol Heart Circ Physiol 286:H847–H855
15. Arac A, Brownell SE, Rothbard JB et al (2011) Systemic augmentation of alphaB-crystallin provides therapeutic benefit twelve hours post-stroke onset via immune modulation. Proc Natl Acad Sci USA 108:13287–13292
16. Ousman SS, Tomooka BH, van Noort JM et al (2007) Protective and therapeutic role for alphaB-crystallin in autoimmune demyelination. Nature 448:474–479
17. Wang J, Martin E, Gonzales V, Borchelt DR, Lee MK (2008) Differential regulation of small heat shock proteins in transgenic mouse models of neurodegenerative diseases. Neurobiol Aging 29:586–597
18. Brownell SE, Becker RA, Steinman L (2012) The protective and therapeutic function of small heat shock proteins in neurological diseases. Front Immunol 3:74
19. Golenhofen N, Bartelt-Kirbach B (2015) HspB5/alpha-B-crystallin in the brain. In: Tanguay RM, Hightower LE (eds) The big book of small heat shock proteins. Springer, Berlin, pp 365–381
20. Wilhelmus MM, Otte-Holler I, Wesseling P et al (2006) Specific association of small heat shock proteins with the pathological hallmarks of Alzheimer's disease brains. Neuropathol Appl Neurobiol 32:119–130
21. Renkawek K, Voorter CE, Bosman GJ, van Workum FP, de Jong WW (1994) Expression of alpha B-crystallin in Alzheimer's disease. Acta Neuropathol 87:155–160

22. Head MW, Corbin E, Goldman JE (1993) Overexpression and abnormal modification of the stress proteins alpha B-crystallin and HSP27 in Alexander disease. Am J Pathol 143:1743–1753
23. Iwaki T, Kume-Iwaki A, Liem RK, Goldman JE (1989) Alpha B-crystallin is expressed in non-lenticular tissues and accumulates in Alexander's disease brain. Cell 57:71–78
24. Iwaki T, Iwaki A, Tateishi J, Sakaki Y, Goldman JE (1993) Alpha B-crystallin and 27-kd heat shock protein are regulated by stress conditions in the central nervous system and accumulate in Rosenthal fibers. Am J Pathol 143:487–495
25. Jellinger KA (2000) Cell death mechanisms in Parkinson's disease. J Neural Transm 107:1–29
26. Gusev NB, Bogatcheva NV, Marston SB (2002) Structure and properties of small heat shock proteins (sHsp) and their interaction with cytoskeleton proteins. Biochemistry (Mosc) 67:511–519
27. Verschuure P, Croes Y, van den IJssel PR et al (2002) Translocation of small heat shock proteins to the actin cytoskeleton upon proteasomal inhibition. J Mol Cell Cardiol 34:117–128
28. Garrido C, Gurbuxani S, Ravagnan L, Kroemer G (2001) Heat shock proteins: endogenous modulators of apoptotic cell death. Biochem Biophys Res Commun 286:433–442
29. Golenhofen N, Arbeiter A, Koob R, Drenckhahn D (2002) Ischemia-induced association of the stress protein alpha B-crystallin with I-band portion of cardiac titin. J Mol Cell Cardiol 34:309–319
30. Golenhofen N, Ness W, Koob R et al (1998) Ischemia-induced phosphorylation and translocation of stress protein alpha B-crystallin to Z lines of myocardium. Am J Physiol 274:H1457–H1464
31. Shao W, Zhang SZ, Tang M et al (2013) Suppression of neuroinflammation by astrocytic dopamine D2 receptors via alphaB-crystallin. Nature 494:90–94
32. Haslbeck M, Franzmann T, Weinfurtner D, Buchner J (2005) Some like it hot: the structure and function of small heat-shock proteins. Nat Struct Mol Biol 12:842–846
33. Sun Y, MacRae TH (2005) The small heat shock proteins and their role in human disease. FEBS J 272:2613–2627
34. Ito H, Okamoto K, Nakayama H, Isobe T, Kato K (1997) Phosphorylation of alphaB-crystallin in response to various types of stress. J Biol Chem 272:29934–29941
35. Chiesa R, Gawinowicz-Kolks MA, Kleiman NJ, Spector A (1987) The phosphorylation sites of the B2 chain of bovine alpha-crystallin. Biochem Biophys Res Commun 144:1340–1347
36. Morrison LE, Hoover HE, Thuerauf DJ, Glembotski CC (2003) Mimicking phosphorylation of alphaB-crystallin on serine-59 is necessary and sufficient to provide maximal protection of cardiac myocytes from apoptosis. Circ Res 92:203–211
37. Li R, Reiser G (2011) Phosphorylation of Ser45 and Ser59 of alphaB-crystallin and p38/extracellular regulated kinase activity determine alphaB-crystallin-mediated protection of rat brain astrocytes from C2-ceramide- and staurosporine-induced cell death. J Neurochem 118:354–364
38. Schmidt T, Bartelt-Kirbach B, Golenhofen N (2012) Phosphorylation-dependent subcellular localization of the small heat shock proteins HspB1/Hsp25 and HspB5/alphaB-crystallin in cultured hippocampal neurons. Histochem Cell Biol 138:407–418
39. Sholl DA (1953) Dendritic organization in the neurons of the visual and motor cortices of the cat. J Anat 87:387–406
40. Dotti CG, Sullivan CA, Banker GA (1988) The establishment of polarity by hippocampal neurons in culture. J Neurosci 8:1454–1468
41. Acunzo J, Katsogiannou M, Rocchi P (2012) Small heat shock proteins HSP27 (HspB1), alphaB-crystallin (HspB5) and HSP22 (HspB8) as regulators of cell death. Int J Biochem Cell Biol 44:1622–1631
42. Head MW, Goldman JE (2000) Small heat shock proteins, the cytoskeleton, and inclusion body formation. Neuropathol Appl Neurobiol 26:304–312
43. van Noort JM, Bsibsi M, Nacken P, Gerritsen WH, Amor S (2012) The link between small heat shock proteins and the immune system. Int J Biochem Cell Biol 44:1670–1679
44. Iwaki T, Kume-Iwaki A, Goldman JE (1990) Cellular distribution of alpha B-crystallin in non-lenticular tissues. J Histochem Cytochem 38:31–39
45. Head MW, Corbin E, Goldman JE (1994) Coordinate and independent regulation of alpha B-crystallin and hsp27 expression in response to physiological stress. J Cell Physiol 159:41–50
46. Head MW, Hurwitz L, Goldman JE (1996) Transcription regulation of alpha B-crystallin in astrocytes: analysis of HSF and AP1 activation by different types of physiological stress. J Cell Sci 109(Pt 5):1029–1039
47. Kato K, Goto S, Hasegawa K, Inaguma Y (1993) Coinduction of two low-molecular-weight stress proteins, alpha B crystallin and HSP28, by heat or arsenite stress in human glioma cells. J Biochem 114:640–647
48. Iwaki T, Iwaki A, Fukumaki Y, Tateishi J (1995) Alpha B-crystallin in C6 glioma cells supports their survival in elevated extracellular K^+: the implication of a protective role of alpha B-crystallin accumulation in reactive glia. Brain Res 673:47–52
49. Iwaki T, Wisniewski T, Iwaki A et al (1992) Accumulation of alpha B-crystallin in central nervous system glia and neurons in pathologic conditions. Am J Pathol 140:345–356
50. Kato S, Hirano A, Umahara T et al (1992) Comparative immunohistochemical study on the expression of alpha B crystallin, ubiquitin and stress-response protein 27 in ballooned neurons in various disorders. Neuropathol Appl Neurobiol 18:335–340
51. Kato S, Hirano A, Umahara T et al (1992) Ultrastructural and immunohistochemical studies on ballooned cortical neurons in Creutzfeldt-Jakob disease: expression of alpha B-crystallin, ubiquitin and stress-response protein 27. Acta Neuropathol 84:443–448
52. Lowe J, Errington DR, Lennox G et al (1992) Ballooned neurons in several neurodegenerative diseases and stroke contain alpha B crystallin. Neuropathol Appl Neurobiol 18:341–350
53. Minami M, Mizutani T, Kawanishi R, Suzuki Y, Mori H (2003) Neuronal expression of alphaB crystallin in cerebral infarction. Acta Neuropathol 105:549–554
54. Bustos FJ, Varela-Nallar L, Campos M et al (2014) PSD95 suppresses dendritic arbor development in mature hippocampal neurons by occluding the clustering of NR2B-NMDA receptors. PLoS One 9:e94037
55. Grabrucker A, Vaida B, Bockmann J, Boeckers TM (2009) Synaptogenesis of hippocampal neurons in primary cell culture. Cell Tissue Res 338:333–341
56. Jaworski J, Spangler S, Seeburg DP, Hoogenraad CC, Sheng M (2005) Control of dendritic arborization by the phosphoinositide-3′-kinase-Akt-mammalian target of rapamycin pathway. J Neurosci 25:11300–11312
57. Niwa M, Hara A, Taguchi A et al (2009) Spatiotemporal expression of Hsp20 and its phosphorylation in hippocampal CA1 pyramidal neurons after transient forebrain ischemia. Neurol Res 31:721–727
58. Irobi J, Almeida-Souza L, Asselbergh B et al (2010) Mutant HSPB8 causes motor neuron-specific neurite degeneration. Hum Mol Genet 19:3254–3265
59. Williams KL, Rahimtula M, Mearow KM (2005) Hsp27 and axonal growth in adult sensory neurons in vitro. BMC Neurosci 6:24

60. Ito H, Kamei K, Iwamoto I et al (2001) Phosphorylation-induced change of the oligomerization state of alpha B-crystallin. J Biol Chem 276:5346–5352
61. Voorter CE, de Haard-Hoekman WA, Roersma ES et al (1989) The in vivo phosphorylation sites of bovine alpha B-crystallin. FEBS Lett 259:50–52
62. Hoover HE, Thuerauf DJ, Martindale JJ, Glembotski CC (2000) alpha B-crystallin gene induction and phosphorylation by MKK6-activated p38. A potential role for alpha B-crystallin as a target of the p38 branch of the cardiac stress response. J Biol Chem 275:23825–23833
63. Launay N, Goudeau B, Kato K, Vicart P, Lilienbaum A (2006) Cell signaling pathways to alphaB-crystallin following stresses of the cytoskeleton. Exp Cell Res 312:3570–3584
64. Adhikari AS, Singh BN, Rao KS, Rao ChM (2011) alphaB-crystallin, a small heat shock protein, modulates NF-kappaB activity in a phosphorylation-dependent manner and protects muscle myoblasts from TNF-alpha induced cytotoxicity. Biochim Biophys Acta 1813:1532–1542
65. Spector A, Chiesa R, Sredy J, Garner W (1985) cAMP-dependent phosphorylation of bovine lens alpha-crystallin. Proc Natl Acad Sci USA 82:4712–4716
66. Renkawek K, Stege GJ, Bosman GJ (1999) Dementia, gliosis and expression of the small heat shock proteins hsp27 and alpha B-crystallin in Parkinson's disease. Neuroreport 10:2273–2276
67. Braak H, Del Tredici K, Sandmann-Kiel D, Rub U, Schultz C (2001) Nerve cells expressing heat-shock proteins in Parkinson's disease. Acta Neuropathol 102:449–454
68. Ecroyd H, Carver JA (2009) Crystallin proteins and amyloid fibrils. Cell Mol Life Sci 66:62–81
69. Wilhelmus MM, Boelens WC, Otte-Holler I et al (2006) Small heat shock proteins inhibit amyloid-beta protein aggregation and cerebrovascular amyloid-beta protein toxicity. Brain Res 1089:67–78
70. Shammas SL, Waudby CA, Wang S et al (2011) Binding of the molecular chaperone alphaB-crystallin to Abeta amyloid fibrils inhibits fibril elongation. Biophys J 101:1681–1689
71. Rekas A, Adda CG, Andrew Aquilina J et al (2004) Interaction of the molecular chaperone alphaB-crystallin with alpha-synuclein: effects on amyloid fibril formation and chaperone activity. J Mol Biol 340:1167–1183
72. Tue NT, Shimaji K, Tanaka N, Yamaguchi M (2012) Effect of alphaB-crystallin on protein aggregation in *Drosophila*. J Biomed Biotechnol 2012:252049
73. Waudby CA, Knowles TP, Devlin GL et al (2010) The interaction of alphaB-crystallin with mature alpha-synuclein amyloid fibrils inhibits their elongation. Biophys J 98:843–851
74. Kulkarni VA, Firestein BL (2012) The dendritic tree and brain disorders. Mol Cell Neurosci 50:10–20
75. Cochran JN, Hall AM, Roberson ED (2014) The dendritic hypothesis for Alzheimer's disease pathophysiology. Brain Res Bull 103:18–28
76. Tanzi RE (2005) The synaptic Abeta hypothesis of Alzheimer disease. Nat Neurosci 8:977–979
77. Terry RD, Masliah E, Salmon DP et al (1991) Physical basis of cognitive alterations in Alzheimer's disease: synapse loss is the major correlate of cognitive impairment. Ann Neurol 30:572–580
78. de Ruiter JP, Uylings HB (1987) Morphometric and dendritic analysis of fascia dentata granule cells in human aging and senile dementia. Brain Res 402:217–229
79. Hanks SD, Flood DG (1991) Region-specific stability of dendritic extent in normal human aging and regression in Alzheimer's disease. I. CA1 of hippocampus. Brain Res 540:63–82